Brain Stimulation 7 (2014) 508–515

Contents lists available at ScienceDirect

Brain Stimulation

journal homepage: www.brainstimjrnl.com

Transcranial Slow Oscillation Stimulation During Sleep Enhances Memory Consolidation in Rats

Sonja Binder [a], Karolin Berg [a], Fernando Gasca [c,d], Belen Lafon [e], Lucas C. Parra [e], Jan Born [a,b], Lisa Marshall [a,c,*]

[a] University of Lübeck, Department of Neuroendocrinology, Lübeck, Germany
[b] University of Tübingen, Institute of Medical Psychology and Behavioral Neurobiology, Tübingen, Germany
[c] University of Lübeck, Graduate School for Computing in Medicine and Life Sciences, Lübeck, Germany
[d] University of Lübeck, Institute for Robotics and Cognitive Systems, Lübeck, Germany
[e] The City College of The City University of New York, Department of Biomedical Engineering, New York, USA

ARTICLE INFO

Article history:
Received 20 December 2013
Received in revised form
24 February 2014
Accepted 1 March 2014
Available online 31 March 2014

Keywords:
Slow oscillation stimulation
tDCS
EEG
Sleep
Memory consolidation

ABSTRACT

Background: The importance of slow-wave sleep (SWS), hallmarked by the occurrence of sleep slow oscillations (SO), for the consolidation of hippocampus-dependent memories has been shown in numerous studies. Previously, the application of transcranial direct current stimulation, oscillating at the frequency of endogenous slow oscillations, during SWS enhanced memory consolidation for a hippocampus dependent task in humans suggesting a causal role of slowly oscillating electric fields for sleep dependent memory consolidation.
Objective: Here, we aimed to replicate and extend these findings to a rodent model.
Methods: Slow oscillatory direct transcranial current stimulation (SO-tDCS) was applied over the frontal cortex of rats during non-rapid eye movement (NREM) sleep and its effects on memory consolidation in the one-trial object-place recognition task were examined. A retention interval of 24 h was used to investigate the effects of SO-tDCS on long-term memory.
Results: Animals' preference for the displaced object was significantly greater than chance only when animals received SO-tDCS. EEG spectral power indicated a trend toward a transient enhancement of endogenous SO activity in the SO-tDCS condition.
Conclusions: These results support the hypothesis that slowly oscillating electric fields causal affect sleep dependent memory consolidation, and demonstrate that oscillatory tDCS can be a valuable tool to investigate the function of endogenous cortical network activity.

Introduction

That sleep promotes memory consolidation for several memory systems was shown in numerous studies in humans and rodents (e.g. Refs. [1–3]). For the consolidation of hippocampus-dependent memories found to benefit from slow-wave sleep [4] an active system consolidation process is assumed based upon the trace transformation theory [5]. Core features of memories that are temporarily encoded into hippocampal networks, are reactivated during SWS to be redistributed toward long-term storage-sites preferentially residing in neocortical areas for long-term maintenance [3,4,6–11]. It is thought that the cortical sleep slow oscillation (SO) with its UP- and DOWN-states, serves as a temporal frame for a hippocampal-neocortical dialogue [12,13]. SOs are coupled in time to hippocampal ripple and thalamic generated spindle activity [12–15], two rhythms also closely associated with memory consolidation during sleep [16,17].

A causal link between slow oscillations during non-rapid-eye movement (NREM) sleep and the consolidation of hippocampus-dependent memories was shown by Ref. [18] in which memory performance was enhanced in humans subsequent to application of

This work was funded by the Deutsche Forschungsgemeinschaft (SFB 654, SPP 1665), the USA-German Collaboration in Computational Neuroscience (German Ministry of Education and Research BMBF, grant 01GQ1008, and grant number NIH-R01-MH-092926-01).
Financial disclosure: The authors declare no competing financial interests.
Parts of this work were presented at the 5th International Conference on Non-Invasive Brain Stimulation, 19–21 March 2013, Leipzig, Germany.
* Corresponding author. University of Lübeck, Department of Neuroendocrinology, Haus 50.1, Ratzeburger Allee 160, 23538 Lübeck, Germany. Tel.: +49 451 500 3644; fax: +49 451 500 3640.
E-mail address: marshall@uni-luebeck.de (L. Marshall).

1935-861X/$ – see front matter © 2014 Elsevier Inc. All rights reserved.
http://dx.doi.org/10.1016/j.brs.2014.03.001

slowly oscillating electric currents (SO-tDCS) during NREM sleep. Yet in elderly, a similar protocol failed to find effects on memory [19]. On the other hand, in the rat SO-tDCS modulated EEG activity and enhanced acquisition in a learning task over multiple days [20]. Relatively weak electric fields resulting from applied weak electric currents can acutely induce effects that are amplified by network interactions and eventually lead to long-lasting changes in bioelectric activity [21–25]. Oscillatory tDCS can modulate ongoing neuronal activity and/or entrain neuronal activity to the applied oscillation; however, the sensitivity of the network and the specific effects depend strongly on the brain state at the time of stimulation [26–32].

Here, we aimed to replicate and extend findings from human subjects on hippocampus-dependent memory consolidation to a rodent model: The stimulation protocol is comparable in mode, intensity and location [33,34], while at the behavioral level a hippocampus-dependent one-trial task (object place recognition, OPR) is employed. Based on our previous findings showing the dependency of this task on sleep containing a large amount of EEG slow wave activity within the retention interval [35,36], we expected memory consolidation to be enhanced after SO-tDCS during slow wave sleep (SWS).

Materials and methods

Animals

Twelve male Long Evans rats (Janvier, Le Genest-Saint-Isle, France), ten to eleven weeks at time of surgery were housed individually with ad libitum access to food and water under a 12 h/12 h light–dark cycle (lights-on 07.00 A.M.). Animals were handled for 7 days prior to surgery. Eleven of the animals took part in a pilot study to find optimal retention intervals for the OPR task. All experimental procedures were performed in accordance with the European animal protection laws and policies (directive 86/609, 1986, European Community) and were approved by the Schleswig–Holstein state authority.

Surgery

Anesthesia and analgesic treatment, EEG and EMG recording, and SO-tDCS electrode application were similar to Ref. [20]. Briefly, for epidural EEG recordings a stainless steel screw-electrode (Plastics One, USA) was placed over the left frontal cortex (AP: +1.6 mm, L: −0.5 mm) and referenced to an occipital site (AP: −12.0 mm; L: ±0.0 mm) using an anterior ground (AP: +6.9, L: +1.1). For bilateral stimulation screw-electrodes (diameter 1.57 mm) were drilled halfway through the skull. Anodes for two separately regulated constant SO-tDCS circuits were positioned over the prefrontal cortex (AP: +2.5 mm, L: ±2.0 mm) and two return electrodes placed over the cerebellum (AP: −10.0 mm, L: ±2.0 mm). Seven days were allowed for recovery.

General procedure and design

On three consecutive days animals were habituated to the empty open-field for 5 min per day. Following habituation, animals' sleep was recorded for 2 h to adapt them to the recording conditions.

The OPR task was conducted similar to Ref. [35]. In brief, each session consisted of a Sample trial (starting around 8 A.M.), followed by a 24 h retention interval, and a Test trial. During the Sample trial two identical objects were positioned in two far corners of the open field (Fig. 1). The rat was put in the center of the open field and explorative behavior in reference to the objects was measured. After 60 s of exploration time across both objects or after reaching the cut-off criterion of 10 min the Sample trial was terminated. The animal was connected to the cables for EEG and stimulation and subsequently brought into the recording box, where it was subjected to either STIM (SO-tDCS) or SHAM (sham-stimulation) during NREM sleep. EEG recordings lasted for 8 h. In the Test trial, the open field contained the same objects as before, but one object was now displaced to another corner. Preference for the displaced object was quantified in the Preference-index, i.e., the quotient of exploration time for the displaced object and total exploration time (exploration of displaced object/[exploration displaced object + exploration stationary object]). A Preference-index > 0.5 indicates a preference for the displaced, a Preference-index <0.5 a preference for the stationary object and 0.5 indicates chance level. Test trial duration was 2 min. Since the preference for the displaced object tends to fade with elapsed time [39] it was calculated for the first Test trial minute and for the entire duration of the Test trial. Positions of objects in Sample and Test trials, and type of object were counterbalanced between conditions. Each rat was tested in two conditions, i.e., an STIM and an SHAM condition, according to a within-subject crossover design. Order of conditions, which were separated by 5–6 days, was counter balanced. Different objects were used in each session. A schematic overview of

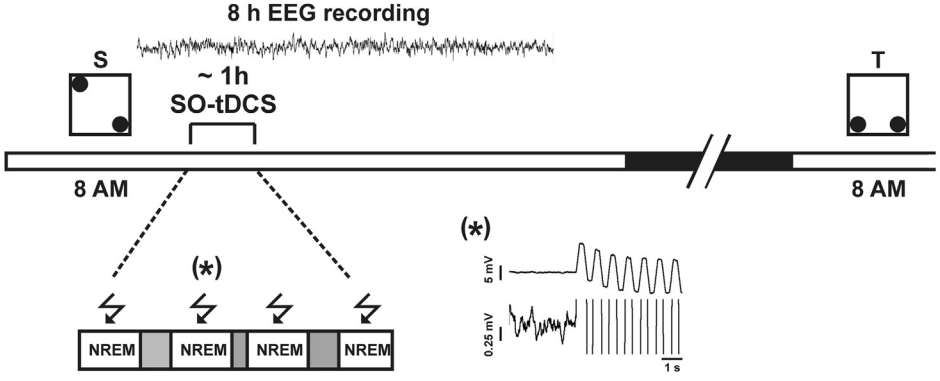

Figure 1. Schema of the experimental procedure. Following completion of the Sample trial (*S*), EEG was recorded for 8 h. After reaching stable NREM sleep (see Materials and methods section for definition), SO-tDCS was applied during NREM sleep only, each stimulation lasting 30 s, separated by at least 30 s. On average, it took ~1 h to reach the desired number of 20 successful stimulations. White bar indicates lights on, black bar lights off. On the bottom right (*), an example of an EEG trace during SO-tDCS is shown. Lower trace and upper trace are identical, but differ in scaling. 24 h after completion of the Sample trial, the Test trial (*T*) was conducted. The signal shift is due to the AC settings of the recording device.

experimental procedures is given in Fig. 1. Sleep recordings were conducted as in Ref. [20].

Behavioral apparatus and objects

Object-place recognition testing took place in a quadratic dark gray open field (80 × 80 cm, 40 cm high, PVC), dimly lit with 11 lux. Behavior was recorded by a camera (model DFK1BU03, The Imaging Source, Bremen, Germany) mounted above the open-field. Camera mounting and surrounding furniture served as putative extra maze cues to facilitate spatial orientation.

Objects were glass bottles of different shape, texture, and size (height 17–26 cm, bottom diameter 6–9 cm), filled each with differently colored sand. Objects and open field were cleaned thoroughly between trials with 60% ethanol solution.

Stimulation parameters

SO-tDCS electrodes were connected through the same swiveling commutator as the EEG and EMG, but through a separate cable to a battery driven constant current stimulator in the adjacent room. For SO-tDCS a current of trapezoid shape, time period corresponding to the frequency range of the sleep slow oscillation (1.33–1.5 Hz), and possessing a DC offset was applied. Current intensity fluctuated between 0 and 9 μA. This maximum current was chosen on the basis of FEM modeling (described below and in the Results section) to reach sufficient fields within the frontal cortex without affecting wide subcortical structures and comparable to current densities used previously [18,27,28,37]. Oscillatory currents were applied to both hemispheres in phase-synchrony. Duration of each stimulation train was 30 s, separated by a stimulation-free period of at least 30 s.

Stimulation started after the first occurrence of 60 s stable NREM sleep and lasted for 30 s, followed by a 30 s stimulation-free interval. If the animals showed signs of awakening during stimulation (movement and/or increased EMG activity), stimulation was terminated, and if any sleep stage change was observed during the stimulation-free period, the next 60 s of stable NREM sleep were awaited before the next stimulation began. Animals received in total 20 stimulations during NREM sleep (prematurely terminated stimulations and those immediately followed by REM or PreREM sleep were repeated). In the SHAM condition, no stimulation was applied, but the EEG recording was marked at respective intervals.

Electric field calculations using the finite element method (FEM)

To estimate the spatial distribution of the electric field magnitude for our electrode positioning at different current intensities, we calculated a realistic 3D model on the bases of Ref. [34]. In brief, data were obtained from an MRI (Phillips Achieva 3T) of an adult living male Wistar rat. Scalp, skull, cerebrospinal fluid (CSF) and brain were subsequently segmented using Simpleware's ScanIP (Simpleware Ltd., Exeter, UK: Fig. 2A).

Calculations of the induced electric field were conducted using the Conductive DC Media module from COMSOL Multiphysics 3.5a (COMSOL AB, Sweden). Given the low stimulation frequencies of SO-tDCS (DC $<$ 2 Hz), the system is considered quasistatic, and tissue is assumed to follow resistivity with no capacitive component. The distribution of the induced electric field was obtained solving Laplace's equation: $\Delta\cdot(\sigma\Delta V)$ where σ is the tissue conductivity and V is the electric potential. The media was considered isotropic using the following electric conductivities: scalp: 0.465 S/m, bone: 0.01 S/m, CSF: 1.65 S/m, brain: 0.2 S/m [38]. For electrodes the distal surface of the anode cylinders was given an

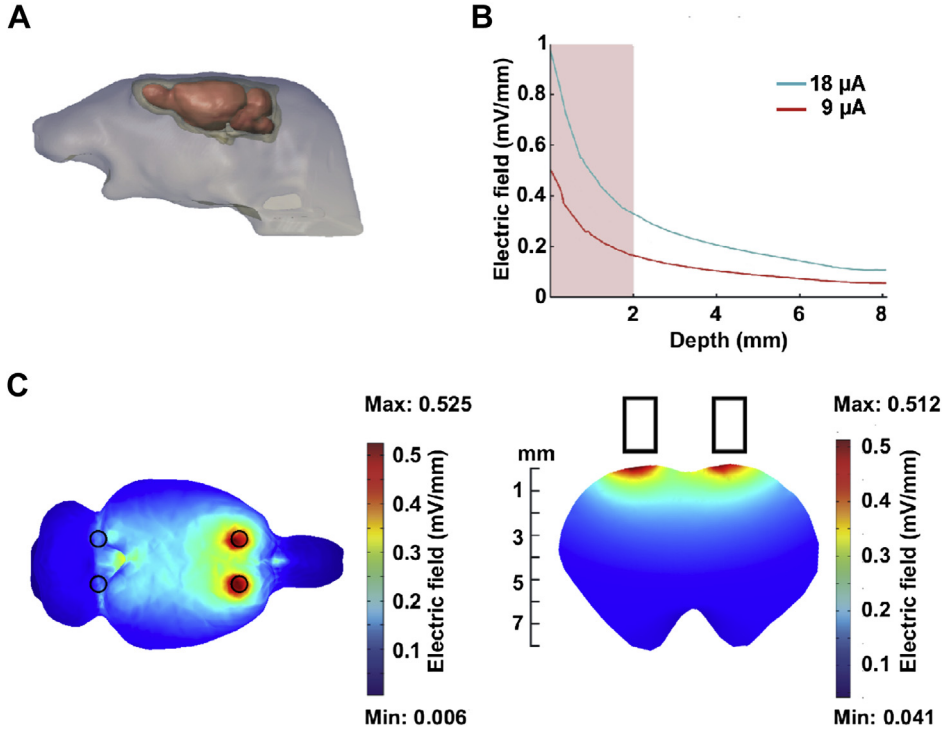

Figure 2. Estimated electric field distributions according to the finite element (FE) rat brain model. A) Anatomically realistic geometries of the rat head model. B) Electric field profile within the brain for two different current strengths; cortical surface corresponds to 0 mm. Pink shaded area represents cortex. C) Electric field distribution (9 μA applied current) on the cortical surface (left) and along a coronal slice positioned at the height of the anodes (right). A detailed description of the FE model is in the methods.

inward current flow J_n (normal current density) of 9 or 18 μA, and the distal surface of the return electrodes was set to zero potential ($V = 0$). The models were composed of ca. 5.7×10^5 tetrahedral elements and 7.9×10^5 degrees of freedom. The resulting induced electric field distributions are shown in Fig. 2B,C.

Data reduction and statistical analyses

Behavioral data

Scoring of recorded explorative behavior was conducted semi-manually using tracking software (ANY-maze, Stoelting Europe, Dublin, Ireland) by an experienced observer blind to the experimental condition according to the above mentioned criteria. The Preference-index (see General procedure and design section) was computed separately for the first and total 2 min of the Test trial [39].

Sleep scoring and sleep architecture

Sleep architecture was determined from EEG and EMG during the first 8 h of the retention interval using 10 s epochs for scoring according to standard criteria [40] with the software SleepSign for Animal (Kissei Comtec, Japan). Stimulation epochs were scored as a separate "stage" (STIM or SHAM), because due to stimulation artifacts a reliable assignment to a distinctive sleep stage could not be guaranteed. In the SHAM condition intervals for sham-stimulation were designated according to the same rules as for real stimulation. Average sleep stages were computed hourly, starting at sleep onset (defined here as the first occurrence of 60 s stable NREM sleep). Furthermore, sleep latency (start of recording until the first occurrence of stable NREM), REM latency and duration of the stimulation period (time from start of the first stimulation to the end of the last stimulation) and total sleep time (TST) were computed.

EEG analysis

Spectral analyses were conducted using custom scripts applying built-in functions of MATLAB (The MathWorks Inc., MA, USA) and the EEGLAB toolbox. Data were first band pass filtered (low pass filter: 35 Hz, 10th order Butterworth; high pass filter: 0.5 Hz, 20th order Butterworth) and subsequently, a Hanning window was applied on blocks of 10,000 sample points (10 s) of EEG data before power spectra were calculated using Fast Fourier Transformations (FFT). Generally, data were normalized using the percentage of each bin (bin size 0.1 Hz) with reference to the total spectral power between 0.8 and 35 Hz. For statistical assessment we analyzed log-powers to account for possible violations of the assumption of normal distribution, following Ref. [41]. Mean spectral power was calculated for all epochs of NREM sleep (i), rapid-eye movement (REM) sleep (ii) and pre-rapid eye movement (PreREM) sleep (iii) after onset of the first (sham-) stimulation for each hour of the entire 8 h recording session. Mean spectral EEG power was furthermore calculated for all epochs of NREM (iv) and REM sleep (v) between the first and the last (sham-) stimulation, and (vi) for a 10 s post-stimulation interval consisting of NREM sleep only and commencing 1 s after the end of stimulation, thereby discarding the stimulation artifact. We choose a 10 s time range since the hypothesized modulation of EEG activity was expected to be strongest immediately following SO-tDCS, similar to previous studies of ours using SO-tDCS [18,20].

Mean spectral power was calculated for the slow oscillation (SO) band (0.8–2.0 Hz), upper delta (2.0–4.0 Hz), theta (5.0–9.0 Hz), and the spindle band (10.5–14.0 Hz). Sleep spindles were detected based on the algorithm used by Ref. [42], see Supplementary text for further information. Spindle density was calculated across all 1 min intervals of NREM sleep for the same time ranges as for the FFT analyses.

Statistics

For statistical analysis, ANOVAs for repeated measures and Student's *t*-tests were used where appropriate. A *P*-value < 0.05 was considered significant. Prior to analyses, data were tested for normal distribution using Shapiro–Wilk tests (all $P > 0.05$). Results are given as means ± SEM unless indicated otherwise.

Results

Estimations of electric field magnitude

As depicted in Fig. 2B,C, the estimated electric field induced by our current of 9 μA was most pronounced directly beneath the electrodes. Field strength per electrode site reached a maximum value of ~0.5 mV/mm at the cortical level, which is slightly below the field of ~0.8 mV/mm induced by endogenous SO activity measured on multi-site recordings from prefrontal cortex in rats (calculations were done on a recording taken from Ref. [43]). Figure 2B shows estimated field strengths for two different current intensities and their decay within deeper brain tissue. Notably, with the applied current of 9 μA a functionally relevant penetration of the induced field to subcortical structures is unlikely, as intended, since we aimed to affect primarily the neocortex.

Memory performance in the test trial

Figure 3 depicts the mean Preference-index for STIM and SHAM in the Test trial following a retention interval of 24 h. The preference for the displaced object was only above the level of chance for the STIM condition (Preference-index during the 1st min and, total 2 min, respectively, for STIM: $T[11] = 3.09$, $P = 0.01$ and $T[11] = 2.42$, $P = 0.034$; for SHAM: $T[11] = 0.65$, $P = 0.53$, $T[11] = 0.22$, $P = 0.83$). Preference-index for the displaced object was significantly higher in the STIM than SHAM condition (Condition [STIM, SHAM]: $F[1,11] = 6.05$, $P = 0.032$; Time [1st min, total 2 min]: $F[1,11] = 0.33$, $P = 0.579$; Condition × Time: $F[1,11] = 0.98$, $P = 0.343$). Thus, only in the STIM condition did animals discriminate between the displaced and stationary objects. Out of the total of 12 animals 9 revealed an increased Preference-index after applying SO-tDCS within the 24 h retention interval. Of the other 3 one performed equally well in both conditions while two showed the opposite pattern, and of these one explored preferentially the non-displaced object in both conditions. In the SHAM condition the Preference-index was

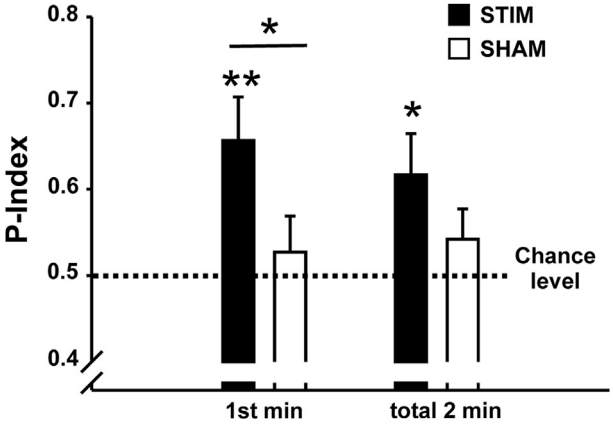

Figure 3. Preference (P)-index (mean ± SEM) for the displaced object during the Test trials for both conditions, separated for the 1st and the total 2 min of the trial. An exploration pattern above chance level is only observed in the STIM condition but not in the SHAM condition. One-sample *t*-tests against chance level and *t*-tests for dependent samples for comparisons between conditions. $^*P < 0.05$, $^{**}P < 0.01$.

equally distributed above and below chance level (Fig. S1A). Exploratory behavior in the Test trials did not differ between the two conditions (total object exploration: STIM: 37.2 ± 3.3 s, SHAM: 37.1 ± 3.9 s, $P = 0.99$).

Within the Sample trials there were no significant differences in object exploration between the two conditions; nor did amount of time spent in the quadrants of the open field during the Test trial indicate any significant object location memory in the SHAM condition (see Supplementary text and Fig. S1B,C for further details).

Brain electric activity during the 8 h recording period

Measures of sleep architecture are depicted in Fig. 4 with an overview of *F*-statistics of the ANOVA results given in Table S1. Across the entire recording period amount of time spent awake, in NREM sleep, PreREM sleep, or total sleep time did not differ significantly between conditions ($P > 0.05$). Animals did spend slightly less time in REM sleep in the STIM condition ($P = 0.016$), but this effect was not statistically maintained for REM sleep as percentage of TST ($P = 0.068$). Also, neither latency to reach stable NREM sleep (STIM: 51.26 ± 3.77 min, SHAM: 52.47 ± 4.69 min, $P > 0.05$) nor percentage of NREM and PreREM sleep differed between conditions. A slight reduction in REM sleep latency following stimulation failed to reach significance (STIM: 62.86 ± 4.14 min, SHAM: 73.22 ± 4.48 min, $P = 0.063$). Total time of the stimulation period was comparable between STIM and SHAM as well (STIM: 55.28 ± 4.87 min, SHAM: 52.5 ± 3.70 min, $P > 0.05$).

EEG power analyzed separately within NREM, REM and PreREM sleep did not differ between conditions for any of the examined frequency bands across the 8 h recording period. Spindle density also did not differ (Table S2, Fig. S2 and Supplementary text).

Brain electric activity within the stimulation-free intervals of SO-tDCS

Signal artefacts due to the trapezoidal pattern of SO-tDCS and, more importantly, due to the frequency overlap of stimulation and endogenous SO activity, precluded EEG analysis in the SO range during acute SO-tDCS. However, Fig. 5A reveals that endogenous SO EEG power (0.8–2 Hz) tended to be enhanced within the first 10 s of the stimulation-free interval in the STIM condition as compared to SHAM ($T[10] = 2.04$, $P = 0.069$) with 8 of the 11 analyzed animals showing this enhancement (Fig. S3A; EEG data of one animal were not included due to excessive artifacts in the above time window). Selective analyses of EEG power within the SO-tDCS frequency range revealed a significant enhancement for STIM (inset in Fig. 5B). Tendency toward EEG power enhancement within this 10 s stimulation-free interval for STIM vs. SHAM does not reflect a random enhancement in SO power within the entire (~1 h) time period, i.e., from the first to last stimulation event (SO: $T[11] = -0.63$, $P = 0.545$). EEG spectral power within the other relevant frequency bands was comparable between STIM and SHAM, both within the 10 s stimulation-free intervals (upper delta: $T[10] = 0.55$, $P = 0.595$; theta: $T[10] = -0.90$, $P = 0.391$; $T[10] = 0.15$, spindle $P = 0.882$) as well as within the entire ~1 h time period (upper delta: $T[11] = -0.36$, $P = 0.725$; theta: $T[11] = 1.29$, $P = 0.225$; spindle: $T[11] = 0.53$, $P = 0.606$; Fig. S3B). Spindle density was not affected by SO-tDCS within the 30 s stimulation-free intervals ($T[11] = -0.38$, $P = 0.708$).

Stimulation epochs

No differences between conditions were found for either the total number of applied (sham) stimulations, including stimulations stopped prematurely or discarded due to sleep stage changes during the acute stimulation (STIM: $M = 23.8 \pm 1.2$, SHAM: $M = 25.3 \pm 0.9$; $P > 0.05$), or for the percentage of stimulations classified as successful (i.e., with continuous NREM sleep immediately after stimulation ended, without any EMG activity or movement during acute SO-tDCS; STIM: $M = 17.8 \pm 0.6$, SHAM: $M = 18.8 \pm 0.2$; $P > 0.05$). Note, deviations in the number of successful stimulations from the desired number of 20 result from this more conservative offline classification.

Discussion

Results reveal an effect of slowly oscillating weak electric current stimulation during early SWS on memory performance in the object-place recognition (OPR) task in the rat: Animals' preference for the displaced object in the memory task was significantly greater than chance after a 24 h retention interval only when animals received SO-tDCS. Although analyses of post-stimulatory EEG slow-oscillatory activity failed to reach significance, there was a tendency toward an enhancement of slow-oscillatory activity within a 10 s interval after cessation of SO-tDCS. It is unlikely that any general difference in sleep architecture contributed to the effect on memory consolidation. The only significant effect involving a slight reduction in REM sleep in the stimulation condition was not maintained when expressed as amount of total sleep time.

The enhancement in sleep-dependent memory consolidation in this and former studies is presumably related to increased synchronization of cortical networks in the SO frequency band which presumably facilitated the hippocampal-neocortical dialogue for memory consolidation [6,9,11–14,44]. Although a proper analysis of cortical activity in the SO frequency range during stimulation is precluded due to artifacts caused by the trapezoidal pattern of SO-tDCS, we were able to measure an increment in SO activity

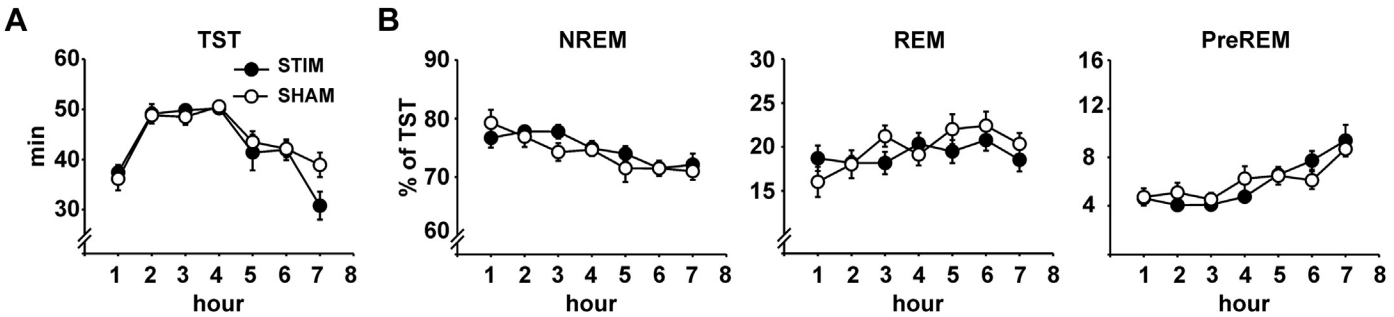

Figure 4. Sleep architecture (mean ± SEM) across the entire recording period within the retention interval. Sleep staging begins after stable NREM sleep was first obtained (on average 52 min after the Test trial). A) Total sleep time (TST) in minutes. B) NREM, REM and PreREM sleep in percentage of TST. Neither TST nor the amount of any sleep stage differed between the conditions.

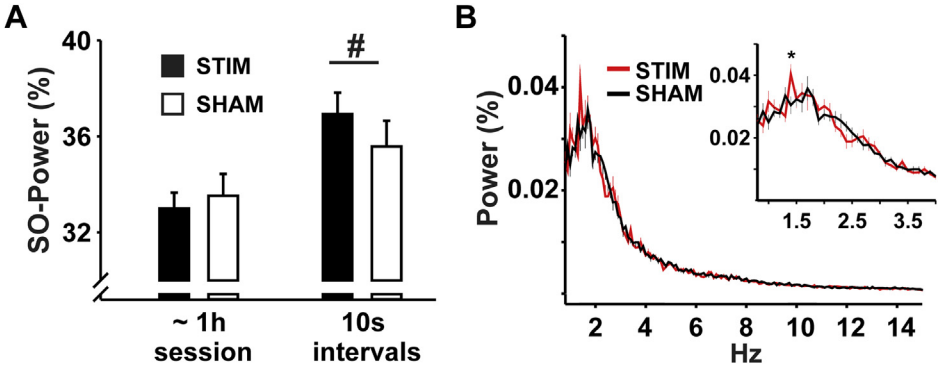

Figure 5. EEG spectral measures during the 10 s post-stimulation interval and the entire ~1 h session from the first to the last (sham) stimulation epoch. Only intervals containing undisturbed NREM sleep were used for analysis. A) Mean spectral power in the SO range (0.8–2 Hz) for the entire time period from the first to the last (sham) stimulation epoch ('~1 h session') and for the mean of all 10 s post-stimulation intervals ('10 s intervals'). SO-power revealed a tendency toward enhancement in the STIM condition during the stimulation-free intervals. $^{\#}P < 0.1$. B) Power spectrum (mean ± SEM) for all animals and intervals ($N = 11$). Power is presented as % of total power between 0.8 and 35 Hz. The inset indicates significance of the relevant frequency bin, $^{*}P < 0.05$.

within the 10 s following stimulation in 8 out of 11 animals. This difference failed, however, to reach statistical significance. Interestingly, the 2 animals which failed to show post-stimulatory enhancement of SO power also performed poorly in the memory test (Preference-index ≤ 0.5).

Our working hypothesis is that SO-tDCS promotes memory consolidation by the same route as endogenous slow oscillation activity. Along this line acute effects on the hippocampo-neocortical system could have occurred here at least on two levels. On the one hand by way of corticofugal connections, SOs could influence hippocampal activity such as sharp-wave ripples [45], which have been shown to play an essential role in memory consolidation [17]. On the other hand, hippocampal inputs may arrive at a neocortex which is more susceptible to these inputs due to enhanced synchronized SO activity and/or modified thalamocortical state [46,47]. In fact the same neuronal ensembles in prefrontal cortex that were active during an actual learning experience were targeted by hippoccampal replay during SWS [48]. Although a direct influence of SO-tDCS on the hippocampus cannot to be completely excluded we estimate this as unlikely. According to our electric field calculations maximum subcortical field strength at the height of the anodes induced by our SO-tDCS was 0.2 mV/mm; comparable fields did not significantly affect hippocampal activity in a similar experimental setup ([27], but see also Ref. [49]).

Cortical SO activity can induce LTP in thalamocortical slice preparations [50] and non-oscillatory cortical polarization can increment plasticity-related substances within the cortex [51–53]. Thus, the effect of SO-tDCS on memory consolidation may have primarily resulted from a topographically focused modulation of plasticity-related substances as a consequence of weak electric stimulation. In fact the efficiency of SO-tDCS at such a long (24 h) retention interval could be viewed as reflecting a strong contribution of cortical network plasticity. Neocortical areas like the medial prefrontal cortex can be recruited for remote memory (i.e., memories which have already become independent of the hippocampus, operationally defined usually as delays > 10 days [54]), as well as for recent spatial memory (still hippocampus dependent memories, usually operationally defined as delays < 3 days [55]). To our knowledge there is no systematic data on the relative contribution of hippocampus and neocortex over time to the one-trial OPR task. Performance maintenance for retention intervals greater than 24 h was only observed for another version of the OPR task using multiple Sample trials over several days [56]. There, memory performance did become independent of the hippocampus over time [57,58].

For our working hypothesis it is relevant that in the rodent, cells in the mPFC fire consistently after hippocampal cells associated with sharp wave ripples in CA1 [46]. It could be argued that the electrode montage used here for SO-tDCS, with two laterally positioned frontal anodal electrodes did not exert its strongest effects on the mPFC region. However, we aimed to enhance and synchronize SO activity not locally, but over a broad area of the frontal cortex. According to the FE model used (Fig. 2), SO-tDCS resulted in an electric field strength which was most intense over superficial primary and secondary motor areas. A specific influence of these motor areas on memory consolidation in the OPR task is unlikely, since no motor learning is required. Furthermore, there was no modification in overall exploratory behavior. Two other studies applying tDCS in rodents have used a unipolar montage and bigger counter electrodes to prevent bypassing of currents [59,60]. However, as suggested by our FE model, the 4 electrode configuration with equally small surface areas used here seems to induce the desired effects with highest current densities beneath the anodes. The increased presence of cerebrospinal fluid under the posterior as compared to the frontal electrodes is responsible for a greater spread of the electric field.

Enhancement of memory consolidation and immediate boosting of SO activity by SO-tDCS applied during early NREM sleep were essentially comparable to effects seen in humans [18]. Even though SO activity was post-stimulatory not enhanced in all animals we take the present findings as suggestive that our behavioral effect was due to a modulation of endogenous SO activity by the applied SO-tDCS. In general, neurons have been shown to synchronize to fields as low as 0.3 mV/mm [61]. Stimulation intensities comparable to or slightly higher than presently employed induced effects such as entrainment of/modulation in unit activity, local field potentials [27,28] and EEG power of faster frequencies [18,20,30], or enhanced EEG coherence [62]. Thus the failure to detect a pronounced effect in the macroscopic EEG could in part be attributed to the relatively borderline putatively induced electric field (~0.5 mV/mm), aimed at mimicking the intensity used in comparable human studies [18,30].

To what extent neocortical MUA may have indeed been modulated by the present parameters of SO-tDCS could not be determined in the framework of the present study, but is relevant for future experiments. Despite other findings on increased spindles after learning in rats [35,42,63] this learning induced increase was not reflected in the present experimental design.

In conclusion, it could be shown that memory effects of SO-tDCS achieved in humans can be successfully transferred to a rodent

model. These findings add evidence to the usefulness of oscillatory tDCS as a tool to investigate the functional relevance of endogenous cortical network activity for cognitive processes.

Acknowledgments

We greatly acknowledge H. Koller from the Electronics Facility at the University of Luebeck for help in designing the stimulation apparatus. We thank Shigeyoshi Fujisawa and György Buzsáki for providing data of intracortical multi-site recordings for electric field calculations and Uwe Melchert (Department of Neuroradiology, University of Luebeck) for technical assistance.

Supplementary data

Supplementary data related to this article can be found at http://dx.doi.org/10.1016/j.brs.2014.03.001.

References

[1] Plihal W, Born J. Effects of early and late nocturnal sleep on declarative and procedural memory. J Cogn Neurosci 1997;9(4):534–47.
[2] Stickgold R. Sleep-dependent memory consolidation. Nature 2005;437(7063):1272–8.
[3] Diekelmann S, Born J. The memory function of sleep. Nat Rev Neurosci 2010;11(2):114–26.
[4] Marshall L, Born J. The contribution of sleep to hippocampus-dependent memory consolidation. Trends Cogn Sci 2007;11(10):442–50.
[5] Winocur G, Moscovitch M, Bontempi B. Memory formation and long-term retention in humans and animals: convergence towards a transformation account of hippocampal-neocortical interactions. Neuropsychologia 2010;48(8):2339–56.
[6] Lesburgueres E, Gobbo OL, Alaux-Cantin S, Hambucken A, Trifilieff P, Bontempi B. Early tagging of cortical networks is required for the formation of enduring associative memory. Science 2011;331(6019):924–8.
[7] Inostroza M, Born J. Sleep for preserving and transforming episodic memory. Annu Rev Neurosci 2013;36:79–102.
[8] Wilson MA, McNaughton BL. Reactivation of hippocampal ensemble memories during sleep. Science 1994;265(5172):676–9.
[9] Takashima A, Petersson KM, Rutters F, et al. Declarative memory consolidation in humans: a prospective functional magnetic resonance imaging study. Proc Natl Acad Sci U S A 2006;103(3):756–61.
[10] Rasch B, Büchel C, Gais S, Born J. Odor cues during slow-wave sleep prompt declarative memory consolidation. Science 2007;315(5817):1426–9.
[11] Gais S, Albouy G, Boly M, et al. Sleep transforms the cerebral trace of declarative memories. Proc Natl Acad Sci U S A 2007;104(47):18778–83.
[12] Sirota A, Csicsvari J, Buhl D, Buzsaki G. Communication between neocortex and hippocampus during sleep in rodents. Proc Natl Acad Sci U S A 2003;100(4):2065–9.
[13] Mölle M, Yeshenko O, Marshall L, Sara SJ, Born J. Hippocampal sharp wave-ripples linked to slow oscillations in rat slow-wave sleep. J Neurophysiol 2006;96(1):62–70.
[14] Mölle M, Eschenko O, Gais S, Sara SJ, Born J. The influence of learning on sleep slow oscillations and associated spindles and ripples in humans and rats. Eur J Neurosci 2009;29(5):1071–81.
[15] Andrillon T, Nir Y, Staba RJ, et al. Sleep spindles in humans: insights from intracranial EEG and unit recordings. J Neurosci 2011;31(49):17821–34.
[16] Fogel SM, Smith CT. The function of the sleep spindle: a physiological index of intelligence and a mechanism for sleep-dependent memory consolidation. Neurosci Biobehav Rev 2011;35(5):1154–65.
[17] Girardeau G, Zugaro M. Hippocampal ripples and memory consolidation. Curr Opin Neurobiol 2011;21(3):452–9.
[18] Marshall L, Helgadottir H, Mölle M, Born J. Boosting slow oscillations during sleep potentiates memory. Nature 2006;444(7119):610–3.
[19] Eggert T, Dorn H, Sauter C, Nitsche MA, Bajbouj M, Danker-Hopfe H. No effects of slow oscillatory transcranial direct current stimulation (tDCS) on sleep-dependent memory consolidation in healthy elderly subjects. Brain Stimul 2013;6(6):938–45.
[20] Binder S, Rawohl J, Born J, Marshall L. Transcranial slow oscillation stimulation during NREM sleep enhances acquisition of the radial maze task and modulates cortical network activity in rats. Front Behav Neurosci 2014;7:220.
[21] Bindman LJ, Lippold OC, Redfearn JW. Long-lasting changes in the level of the electrical activity of the cerebral cortex produced bypolarizing currents. Nature 1962;196:584–5.
[22] Weiss SA, Faber DS. Field effects in the CNS play functional roles. Front Neural Circuits 2010;4:15.
[23] Anastassiou CA, Montgomery SM, Barahona M, Buzsaki G, Koch C. The effect of spatially inhomogeneous extracellular electric fields on neurons. J Neurosci 2010;30(5):1925–36.
[24] Marquez-Ruiz J, Leal-Campanario R, Sanchez-Campusano R, et al. Transcranial direct-current stimulation modulates synaptic mechanisms involved in associative learning in behaving rabbits. Proc Natl Acad Sci U S A 2012;109(17):6710–5.
[25] Buzsaki G, Anastassiou CA, Koch C. The origin of extracellular fields and currents–EEG, ECoG, LFP and spikes. Nat Rev Neurosci 2012;13(6):407–20.
[26] Kirov R, Weiss C, Siebner HR, Born J, Marshall L. Slow oscillation electrical brain stimulation during waking promotes EEG theta activity and memory encoding. Proc Natl Acad Sci U S A 2009;106(36):15460–5.
[27] Ozen S, Sirota A, Belluscio MA, et al. Transcranial electric stimulation entrains cortical neuronal populations in rats. J Neurosci 2010;30(34):11476–85.
[28] Fröhlich F, McCormick DA. Endogenous electric fields may guide neocortical network activity. Neuron 2010;67(1):129–43.
[29] Marshall L, Binder S. Contribution of transcranial oscillatory stimulation to research on neural networks: an emphasis on hippocampo-neocortical rhythms. Front Hum Neurosci 2013;7:614.
[30] Antonenko D, Diekelmann S, Olsen C, Born J, Mölle M. Napping to renew learning capacity: enhanced encoding after stimulation of sleep slow oscillations. Eur J Neurosci 2013;37(7):1142–51.
[31] Merlet I, Birot G, Salvador R, et al. From oscillatory transcranial current stimulation to scalp EEG changes: a biophysical and physiological modeling study. PLoS One 2013;8:e57330.
[32] Ali MM, Sellers KK, Fröhlich F. Transcranial alternating current stimulation modulates large-scale cortical network activity by network resonance. J Neurosci 2013;33(27):11262–75.
[33] Brown VJ, Bowman EM. Rodent models of prefrontal cortical function. Trends Neurosci 2002;25(7):340–3.
[34] Gasca F, Marshall L, Binder S, Schlaefer A, Hofmann UG, Schweikard A. Finite element simulation of transcranial current stimulation in realistic rat head model. Neural Engineering (NER), 5th International IEEE/EMBS Conference on; 2011. pp. 36–9.
[35] Binder S, Baier PC, Mölle M, Inostroza M, Born J, Marshall L. Sleep enhances memory consolidation in the hippocampus-dependent object-place recognition task in rats. Neurobiol Learn Mem 2012;97(2):213–9.
[36] Inostroza M, Binder S, Born J. Sleep-dependency of episodic-like memory consolidation in rats. Behav Brain Res 2013;237:15–22.
[37] Reato D, Gasca F, Datta A, Bikson M, Marshall L, Parra LC. Transcranial electrical stimulation accelerates humansleep homeostasis. PLoS Comput Biol 2013;9(2):e1002898.
[38] Datta A, Bansal V, Diaz J, Patel J, Reato D, Bikson M. Gyri-precise head model of transcranial direct current stimulation: improved spatial focality using a ring electrode versus conventional rectangular pad. Brain Stimul 2009;2(4):201–7. 207.
[39] Dix SL, Aggleton JP. Extending the spontaneous preference test of recognition: evidence of object-location and object-context recognition. Behav Brain Res 1999;99(2):191–200.
[40] Neckelmann D, Olsen OE, Fagerland S, Ursin R. The reliability and functional validity of visual and semiautomatic sleep/wake scoring in the Moll-Wistar rat. Sleep 1994;17(2):120–31.
[41] Gasser T, Bacher P, Mocks J. Transformations towards the normal distribution of broad band spectral parameters of the EEG. Electroencephalogr Clin Neurophysiol 1982;53(1):119–24.
[42] Eschenko O, Mölle M, Born J, Sara SJ. Elevated sleep spindle density after learning or after retrieval in rats. J Neurosci 2006;26(50):12914–20.
[43] Fujisawa S, Buzsaki GA. 4 Hz oscillation adaptively synchronizes prefrontal, VTA, and hippocampal activities. Neuron 2011;72(1):153–65.
[44] Ngo HV, Martinetz T, Born J, Mölle M. Auditory closed-loop stimulation of the sleep slow oscillation enhances memory. Neuron 2013;78(3):545–53.
[45] Isomura Y, Sirota A, Ozen S, et al. Integration and segregation of activity in entorhinal-hippocampal subregions by neocortical slow oscillations. Neuron 2006;52(5):871–82.
[46] Wierzynski CM, Lubenov EV, Gu M, Siapas AG. State-dependent spike-timing relationships between hippocampal and prefrontal circuits during sleep. Neuron 2009;61(4):587–96.
[47] Mölle M, Bergmann TO, Marshall L, Born J. Fast and slow spindles during the sleep slow oscillation: disparate coalescence and engagement in memory processing. Sleep 2011;34(10):1411–21.
[48] Peyrache A, Khamassi M, Benchenane K, Wiener SI, Battaglia FP. Replay of rule-learning related neural patterns in the prefrontal cortex during sleep. Nat Neurosci 2009;12(7):919–26.
[49] Reato D, Rahman A, Bikson M, Parra LC. Low-intensity electrical stimulation affects network dynamics by modulating population rate and spike timing. J Neurosci 2010;30(45):15067–79.
[50] Chauvette S, Seigneur J, Timofeev I. Sleep oscillations in the thalamocortical system induce long-term neuronal plasticity. Neuron 2012;75(6):1105–13.
[51] Islam N, Aftabuddin M, Moriwaki A, Hattori Y, Hori Y. Increase in the calcium level following anodal polarization in the rat brain. Brain Res 1995;684(2):206–8.
[52] Islam N, Moriwaki A, Hattori Y, Hayashi Y, Lu YF, Hori Y. c-Fos expression mediated by N-methyl-D-aspartate receptors following anodal polarization in the rat brain. Exp Neurol 1995;133(1):25–31.

[53] Moriwaki A. Polarizing currents increase noradrenaline-elicited accumulation of cyclic AMP in rat cerebral cortex. Brain Res 1991;544(2):248–52.
[54] Frankland PW, Bontempi B. The organization of recent and remote memories. Nat Rev Neurosci 2005;6(2):119–30.
[55] Leon WC, Bruno MA, Allard S, Nader K, Cuello AC. Engagement of the PFC in consolidation and recall of recent spatial memory. Learn Mem 2010;17(6):297–305.
[56] Gaskin S, Gamliel A, Tardif M, Cole E, Mumby DG. Incidental (unreinforced) and reinforced spatial learning in rats with ventral and dorsal lesions of the hippocampus. Behav Brain Res 2009;202(1):64–70.
[57] Gaskin S, Tardif M, Mumby DG. Prolonged inactivation of the hippocampus reveals temporally graded retrograde amnesia for unreinforced spatial learning in rats. Neurobiol Learn Mem 2011;96(2):288–96.
[58] Gaskin S, Tardif M, Mumby DG. Patterns of retrograde amnesia for recent and remote incidental spatial learning in rats. Hippocampus 2009;19(12):1212–21.
[59] Liebetanz D, Koch R, Mayenfels S, König F, Paulus W, Nitsche MA. Safety limits of cathodal transcranial direct current stimulation in rats. Clin Neurophysiol 2009;120(6):1161–7.
[60] Dockery CA, Liebetanz D, Birbaumer N, Malinowska M, Wesierska MJ. Cumulative benefits of frontal transcranial direct current stimulation on visuo-spatial working memory training and skill learning in rats. Neurobiol Learn Mem 2011;96(3):452–60.
[61] Francis JT, Gluckman BJ, Schiff SJ. Sensitivity of neurons to weak electric fields. J Neurosci 2003;23(19):7255–61.
[62] Strüber D, Rach S, Trautmann-Lengsfeld SA, Engel AK, Herrmann CS. Antiphasic 40 Hz oscillatory current stimulation affects bistable motion perception. Brain Topogr 2014;27(1):158–71.
[63] Fogel SM, Smith CT, Beninger RJ. Evidence for 2-stage models of sleep and memory: learning-dependent changes in spindles and theta in rats. Brain Res Bull 2009;79(6):445–51.